Pires et al. Pleistocene megafaunal interaction networks became more vulnerable after human arrival

SUPPLEMENTARY MATERIAL

Appendix S1

Appendix S2

Figures S1-S8

Tables S1-S8

APPENDIX S1. Inferring predator-prey interactions and the cross-validation of our models

Palaeodietary inferences may be based on a diverse array of methods such as indirect evidence of interactions [1], functional morphological analysis [2], and stable isotope analysis [3]. Moreover, there is a lot of information available on the diet of extant mammals and in some cases we might be able to infer diets of extinct species from the diets of their close extant relatives. Yet, we also know diets change over time and across space and depend on population densities, being context-dependent [4]. For this reason, instead of extrapolating what we know from modern systems, or from an often incomplete set of species from specific Pleistocene sites to reconstruct Pleistocene networks, we used a probabilistic model, which allows building networks that incorporate biological realism and our uncertainty on the interactions that happened in the past. We then cross-validate this probabilistic approach with information from different approaches used to infer palaeodiets.

The dietary reconstructions we obtained based on body mass relationships are congruent with dietary studies using other methods. For instance, isotope analyses of

large carnivores in the La Brea region suggest *Smilodon fatalis* and *Panthera leo atrox* preyed upon ruminant and nonruminant species, including bisons [5], whereas *Canis dirus* preyed upon horses more often than on large camelids and bisons [6]. Indirect evidence of predation, as suggested by a damaged skull, indicates that *S. fatalis* could also take down glyptodontids [7]. Isotopes also indicate the South American saber-toothed cat, *Smilodon populator*, preyed upon ground sloths and *Macrauchenia* in South America and the Pleistocene South American jaguar, *Panthera onca mesembrina*, consumed horses and camelids [8]. On the other hand, ecomorphological analyses indicates that *Theriodictis tarijensis* [9] and other South American canids [10] probably consumed smaller prey such as cervids, giant rodents and camelids. Accordingly the probabilistic model we used to reconstruct Pleistocene networks often assigned high probabilities for these interactions inferred by distinct palaeoecological approaches.

Our approach using body mass relationship also reproduces the dietary patterns of living species that were present in Pleistocene assemblages. For instance, most studies suggest cougars (*Puma concolor*) in North America hunt preferentially medium-sized prey such as elk (*Cervus canadensis*), mule deer (*Odocoileus hemionus*) and pronghorn (*Antilocapra americana*) [11, 12]. Accordingly, our model predicts that the probability of an interaction between cougars and herbivores within this size range is high. Similarly, the model assigns high probability for the interactions between the jaguar (*Panthera onca*) and prey on the size range of peccaries (Tayassuidae), capybaras (*Hydrochoerus hydrochaeris*) and deer (*Mazama* spp.), which are among the main prey of extant jaguars [13, 14].

In addition to predicting specific species interactions, the networks generated by our models (Figure S1) reproduce some community-level patterns inferred using other

approaches. The reconstructed Pleistocene networks are characterized by (i) high dietary overlap among predators, (ii) large predators with broad diets and smaller predators with more restricted diets, (iii) and fewer interactions between carnivores and the largest herbivores. All these general patterns are cross-validated by other approaches often used to infer palaeoecology of Pleistocene mammals

High dietary overlap: Isotopic analyses of Pleistocene mammals from Rancho la Brea suggested high dietary overlap among carnivores as yielded by our approach [5]. These results are congruent with the morphological evidence suggesting competition between large carnivores in several North American sites [15]. Along the same lines, palaeoecological inferences based on isotope analysis and ecomorphology for South American megafauna suggest large carnivores such as the *Smilodon* and the jaguar had overlapping diets [8, 10].

The diet of large predators: The prediction that large carnivores would prey on herbivores with variable body size is corroborated by reconstructions of the diets of Pleistocene carnivores in Eastern Beringia using stable isotopes, which suggest large carnivores had varied diets consuming both the largest prey and smaller species [4, 16]. Accordingly isotope and functional morphology analyses suggest that South American *Smilodon populator* and the jaguar had broad diets that include smaller prey such as small camelids and large prey such giant sloths [8, 10].

Low predation of the largest herbivores: All the studies above also suggest the largest herbivores were consumed less often, which is also recovered in our reconstructed networks based on body size relationships. For example, isotopic and functional morphology analyses support the notion that ground sloths were likely to be prey of just a small subset of the predator coterie in South America. In contrast, small camelids were consumed by a greater diversity of predators [8, 10].

To sum up, previous work on the palaeoecology of North and South American Pleistocene assemblages suggest our approach using body mass relationships under a probabilistic framework results in realistic reconstructions of predator-prey interactions between Pleistocene mammals.

APPENDIX S2. Supplementary Methods

Probabilistic Niche Model (PNM)

In the PNM species are ordered along an axis representing a niche dimension and a predator preys upon species within a determined diet range along this axis. The probability of an interaction between consumer *i* and resource *j* is a continuous function:

$$P(i,j \mid \theta) = v \exp\left\{-\left(\frac{n_j - c_i}{r_i}\right)^2\right\} \quad (6)$$

where n_j represents the position in the niche dimension for prey *j*, c_i represents the diet optimum of predator *i*, r_i is the diet range for predator *i*, and v is the maximum probability that *i* consumes any given prey, here set as $v = 1$ following Williams et al. [17]. In our analysis species can be only predators or prey; thus, species positions (n) are defined only for the prey species, whereas diet center and ranges (c and r) are defined only for the predators [18]. To parameterize the model using body mass information we followed Williams et al. [17] and set $n = (\log m_j - \log m_{min})/(\log m_{max} - \log m_{min})$, where m_j is the body mass of prey species *j* and m_{min} and m_{max} are the minimum and maximum values for prey body mass. The parameters r_i and c_i are free parameters. Thus, the free parameter set can be defined as $\theta = \{c_1, c_2, \ldots c_P, r_1, r_2, \ldots r_P\}$.

Assigning interaction strengths

In the baseline analyses off-diagonal elements of community matrix **Q**, q_{ij}, were only $\neq 0$ if $a_{ij} = 1$, thus using the reconstructed networks as backbones. Diagonal elements of **Q**, were always assigned values < 0, representing the negative effect of intraspecific competition. We used different methods to assign values to matrix **Q**. The method used in the baseline analyses is similar to previous work on the stability of food webs [19]. Each matrix cell $q_{ij} \neq 0$ was assigned a value x_{ij} drawn from a normal distribution with parameters $\mu = 1$ and $\sigma = 1$. Because prey have positive effects on the demography of predators, but predators have negative effects on prey populations, we used $-|x_{ij}|$ when q_{ij} represented the effect of predator i on prey j and $|x_{ji}|$ for the effect of prey j on predator i. Note that q_{ij} and q_{ji} are sampled independently. We chose a Gaussian distribution centred around 1 because it guarantees that most of the values will be small while only a few will be large, a pattern that is often found in nature [20]. To test the sensitivity of our results to parameterization we reran analyses varying both μ (from 0 to 5.0 by 0.1) and σ (0.1 to 2.0 by 0.1). Although low variance in interaction strengths (low values for σ) tends to generate only stable matrices the results of those sensitivity tests suggest the parameters of the distribution have little effect on the qualitative patterns we found, since the assemblages with the largest and smallest P_{st} were consistently the same over the ranges of the parameters (Figure S8). Moreover, similar to the results of Allesina and Tang [19] on the consequences of using different distributions for interaction strengths, exploratory analyses where we varied the distribution of interaction strengths showed that different distributions also yield qualitatively similar results. We explored two additional methods for assigning interaction strengths: one

where the per capita effect of predators on prey is greater than the effect of prey on predators and the other assuming interaction strengths also depend on body mass relationships (see below).

Asymmetry in the distribution of interaction strengths. The efficiency of predators in converting prey into actual population growth is unlikely to be close to maximum. Thus the per capita effect of the prey on the predator may be smaller than the converse. Several studies on food web dynamics have considered this asymmetry in interaction strengths [21, 22]. To test the effect of breaking the symmetry between the distributions of interaction strengths we reran all tests assuming the average per capita effects of predators upon their prey are twice as large as the effect of prey on predators. We did this by drawing interaction strengths from different distributions ($\mu_1 = \mu_2/2$). Breaking the symmetry in interaction strength distributions did not alter the results qualitatively (Tables S3-S6).

Interaction strength as a function of body mass. If we assume the body-size relationship between predator and prey determines the probability of interactions, it may affect the demographic effect of interactions as well [23, 24]. Therefore we tested the effects of assigning interaction strengths in matrix **Q** as a function of body-size relationships by defining the off-diagonal elements as:

$$q_{ij} = a_{ij} y_{ij} e^{-\left(m_i - m_j\right)^2} \quad (7),$$

where the term y_{ij} is a random value drawn from a normal distribution with parameters $\mu = 1$ and $\sigma = 1$. This formulation was adapted from studies on coevolution that model the evolutionary outcomes of species interactions taking into account phenotype matching [25, 26]. Such a formulation implies smaller interaction effects for species

that differ in size by a great amount. The random variable y_{ij} adds noise to the relationship and portrays the uncertainty about how exactly body-mass relationships translate into interaction strengths. By considering the uncertainty of the relationship between body mass and interaction effects, we loosen the constraints imposed by body size. In this way we allow, for instance, that large prey benefits small predators, as would be expected for predators that also feed on carcasses [27] or social predators, such as lions and wolves, which are able to prey upon larger prey [28].

Assigning interactions strengths as a function of body-mass relationships reproduces patterns that are more realistic for large-mammal assemblages: large-sized predators will have a stronger impact on populations of medium–sized prey, smaller predators will have larger effects on small prey, and the largest prey are controlled mainly by bottom-up effects [29]. It also increases compartmentalization since predators will tend to interact more heavily with prey within a certain size range [30]. Nevertheless, changing the way we assign interaction strength does not alter the results on P_{st} and τ (Tables S3-S6).

Influence of humans over other predators. Besides the effects of predation on herbivores and indirect effects on predators via indirect competition, humans had the potential to directly interfere with the populations of predators by killing them, chasing them out or scavenging other predator kills as happens with modern societies [31]. To test how this potential interference could influence our results we randomly assigned interactions between added humans and the other predators. We tested three different scenarios by changing the mean of probability distributions used to sample interaction strengths so that the mean negative impact of humans over predators was (i) half, (ii) equal, (iii) or twice as large as the mean impact of predators on

herbivores. Our results show that adding these direct effects of humans over predator populations lead to the same results found with the baseline analyses (Figure S7).

Stability of feasible equilibrium points under a specific dynamical model

In the baseline analyses we examine the stability of a large number of possible community matrices without assuming a particular underlying model [19]. This allowed us to investigate how the combination of species richness and expected network topology for each site would affect dynamics without constraints of the assumptions of a particular dynamic model. However, by doing so we could not evaluate the feasibility of analysed equilibrium points [32]. An equilibrium point can be considered feasible when all species have equilibrium densities, $X^* > 0$ [22]. To check whether our results are consistent when we consider only feasible equilibrium points we analysed the dynamics of large-mammal assemblages while assuming a linear Lotka-Volterra model. Although the Lotka-Volterra model is simple it has the convenient feature that their equilibrium dynamics are well understood. Moreover, assuming a Lotka-Volterra model the elements of the community matrix **Q** can be obtained in terms of biologically meaningful parameters [22].

In a Lotka-Volterra framework, population density (X) increases or decrease with an intrinsic rate (r) and responds linearly to the density of other species:

$$\frac{dX_i}{dt} = X_i\left(r_i + \sum_{j=1}^{n} b_{ij}X_j\right) \quad (8)$$

Assuming matrix **B** is a matrix containing the interaction coefficients b_{ij}, the elements of the community matrix are [22, 33]:

$$q_{ij} = b_{ij}X_i^* \quad (9)$$

Equilibrium densities can be obtained from the intrinsic rates of increase, r, and the inverse of **B**:

$$X^* = -\mathbf{B}^{-1}r \quad (10)$$

We used the probability of interactions, p_{ij}, computed using the LRM to obtain estimates of interaction coefficients. We defined $b_{ij} = p_{ij} \times y_{ij}$, where Y is a random variable with normal distribution, and portrays uncertainty on the true relationship between the probability of interactions and interaction coefficients. Because the benefit predators earn from captured prey depends on their effectiveness in converting prey into biomass [21], we assume $Y \sim N(1, 0.5)$ for predator effects upon prey and $Y \sim N(0.1, 0.5)$ for prey effects upon predators. We used species body mass to obtain estimates of intrinsic growth rates following Weitz and Levin [34]:

$$r = k \times m^{-1/4} \quad (11)$$

Intrinsic growth rates are always positive for prey and negative for predators, representing predator mortality rate [22]. Therefore smaller-bodied herbivores have higher growth rate whereas smaller-bodied predators have higher mortality. We fixed $k = 10$ for prey species and $k = 1$ for predators so that mortality was small relative to the growth rate of prey.

We started each simulation by building the matrix **B** and then used b_{ij} and r estimates to compute equilibrium densities, using eq. 10, for all species in a given site. We discarded all simulations resulting in unfeasible communities ($X_i^* \leq 0$ for any species i) and built the community matrix **Q**, using eq. 9, for the first 10,000 feasible **Q** representing each site. Finally, we assessed the stability of each feasible equilibrium point by analysing $\lambda_{\mathbb{R}}$ for each **Q** matrix. We repeated all previous steps for all analysed sites and analysed 10,000 scenarios per site to compute mean P_{st} and confidence intervals. To investigate the congruence between the results obtained

using this specific dynamic model and the method used for the baseline analyses we tested the determinants of P_{st} (see below) and the correlation between the P_{st} estimates obtained for the baseline analyses and the analysis using this specific dynamical model. Results are in Table S5 and S6 and Figure S3.

Assemblage composition and dynamics

To evaluate which components determining community structure are the most important in determining the dynamic behaviour of the predator-prey systems we used regression models of the form:

$$P_{st} = \beta_0 + \beta_1 \times K_{pred} + \beta_2 \times K_{pred} + \beta_3 \times m_{pred} + \beta_4 \times m_{prey} + \beta_5 \times N^* + \beta_6 \times M^* + \varepsilon, \quad (12)$$

where β_i are partial coefficients of the model, K_{pred} and K_{prey} are the richness of predator and prey species, m_{pred} and m_{prey} are the average body mass of predators and prey species, N^* and M^* are the average relative nestedness and modularity and ε is the usual Gaussian error. We also used a similar model to test how each factor affected τ. We use the relative values of nestedness and modularity to control for the relationship between network size and the two metrics. All models passed diagnostic tests, performed using R [35], to check whether the assumptions of general linear tests such as homogeneity of variances and normality of errors applied for each model. We used the AIC to select among models including different combinations of explanatory variables. In Tables S5 and S6, for the models with best relative goodness of fit (lowest AIC value), we report the results of the regression analyses for P_{st} and τ for each different method used to assign interaction strengths. The results are qualitatively similar irrespective of the method used to assign interaction strengths: greater predator richness decreases P_{st} and increases τ and larger average prey body mass increases P_{st} and decreases τ.

Testing the reliability of P_{st} estimates

It is unlikely that dynamical systems like assemblages of interacting species have only one feasible equilibrium point [19]. Because we built one community matrix **Q** from each interaction matrix **A** generated using the body-mass parameterized model, we are analysing only one of the possible equilibrium points of each system. To test whether this approach impacted the patterns we found, we generated 100 possible matrices **Q** using each of 100 matrices **A** as a template in a total of 10,000 **Q** matrices. We then looked at the real part of the leading eigenvalue of each of the 100 **Q** matrices generated from **A** to determine the probability of stability, P_{st}, of **A.** By doing this we explored distinct possible equilibrium points for each possible structure. We then tested whether the averaged P_{st} over the 100 **A** matrices differed from the P_{st} computed by considering only one equilibrium point for each matrix **A**. As seen in Table S8, these two approaches yield very similar results.

Pleistocene African assemblages

The LQE was not as severe in Africa as it was in the other continents [36]. Thus, in the baseline simulations we compared the network structure and dynamic properties of Pleistocene assemblages against modern African assemblages. Yet, palaeontological data show that some extinctions of large mammals did occur close to the Pleistocene-Holocene boundary in Africa [36, 37]. We tested whether our results on the effect of humans over community stability were robust when considering extinct African mammals as part of African large-mammal assemblages. Because sites with complete late Pleistocene assemblages are scant in Africa we assembled data on the late Pleistocene large-mammal fauna of Southern and Eastern Africa

(Table S7), added extinct species to the African assemblages of our original data set, and reran the analysis on the effect of humans.

Supplementary Figures

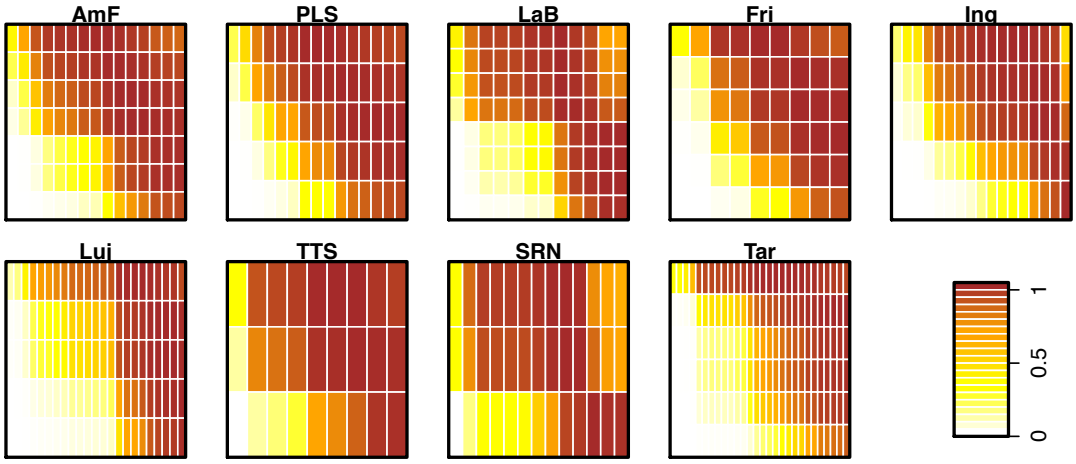

Figure S1 Interaction matrices representing each Pleistocene site. Rows represent predators, ordered from the largest (top) to the smallest (bottom). Columns represent prey ordered from the largest (left) to the smallest (right). The colour heat in each matrix element represents the probability of each interaction. Information on each species can be found in Supplementary Data S1.

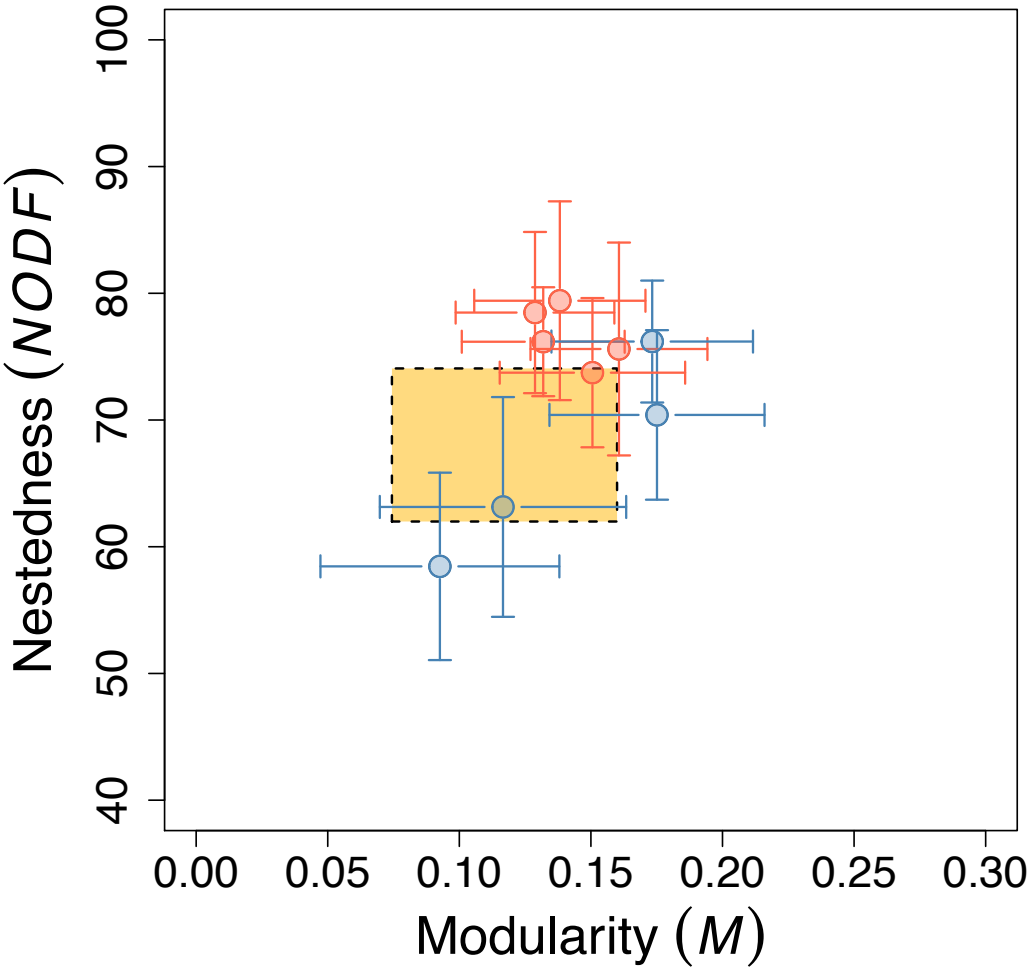

Figure S2 Average degree (±SD) of nestedness (*NODF*) and modularity (*M*) of reconstructed Pleistocene predator-prey networks. The limits of the yellow rectangle define the range of values for modern African assemblages. Red and blue points refer to North and South American sites respectively.

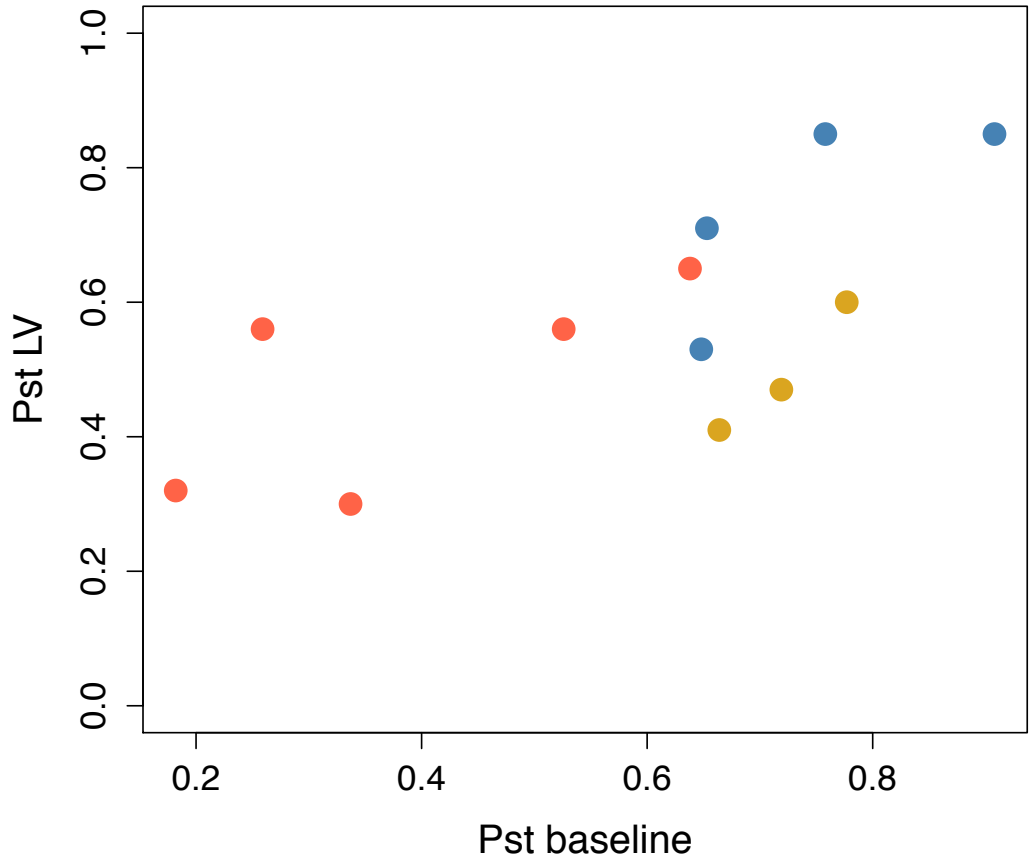

Figure S3 Mean estimated probability of stability, P_{st}, when considering only feasible equilibrium points under a Lotka-Volterra model versus mean P_{st} obtained in the baseline analyses. Pearson correlation test: $r = 0.68$; $p < 0.05$.

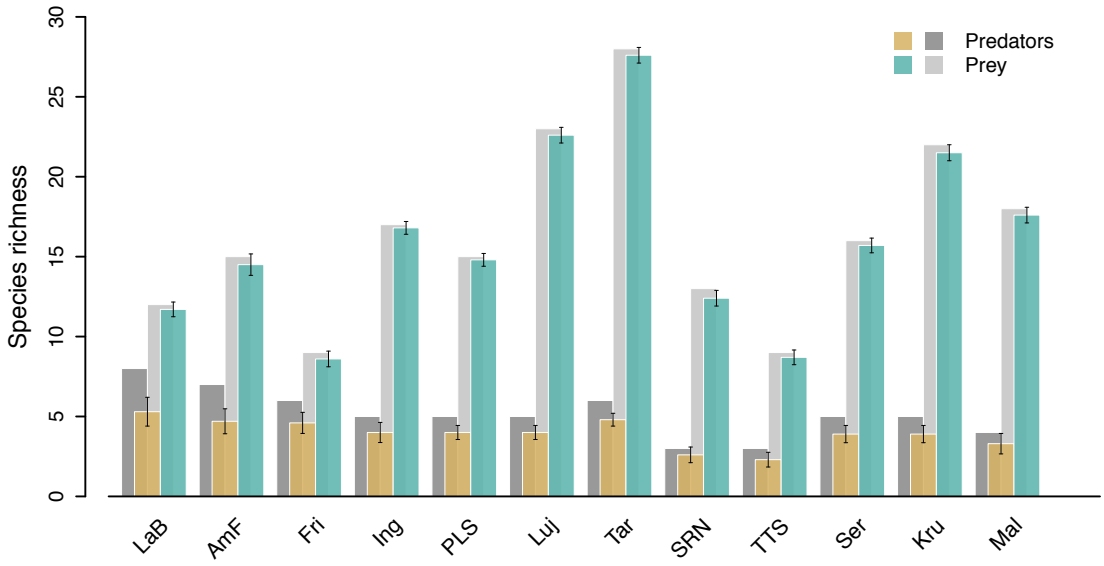

Figure S4 Smallest changes in species composition resulting in the largest change in stability properties for each site. Grey bars depict the original number of predators and prey in each site. Coloured bars show the average number of predators and prey after extinction simulations. Error bars tied to the coloured bars denote the standard deviation for 100 extinction simulations.

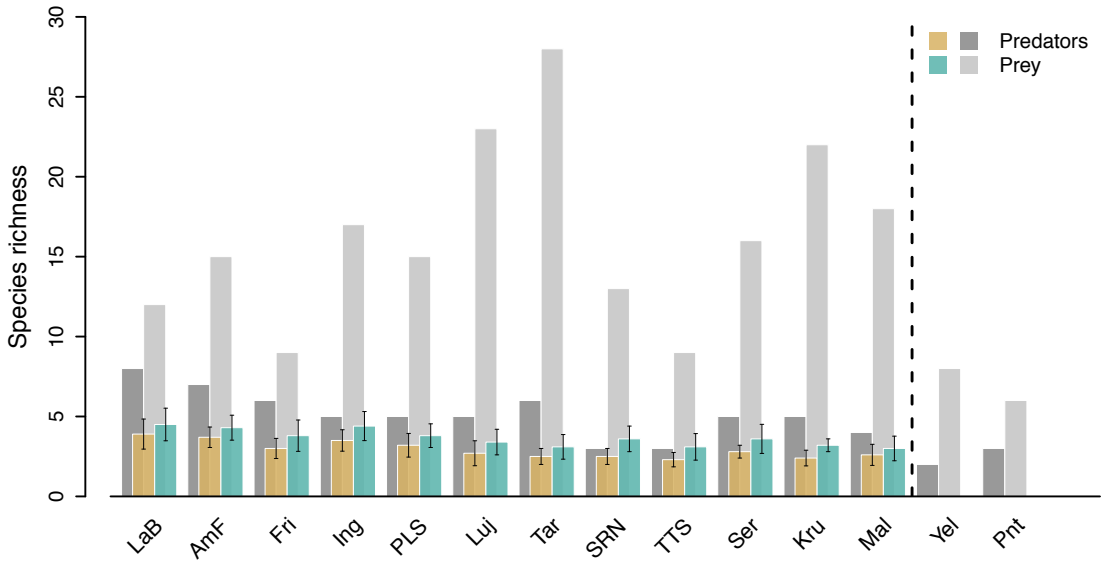

Figure S5 Changes in species composition resulting in the most resilient communities for each site. Grey bars depict the original number of predators and prey in each site. Coloured bars show the average number of predators and prey after extinction simulations. Error bars tied to the coloured bars denote the standard deviation for 100 extinction simulations. The bars on the right side of the dashed line show the number of predators and prey species in two sites with relatively rich mammalian faunas in North and South America today (Yel = Yellowstone; Pnt = Pantanal).

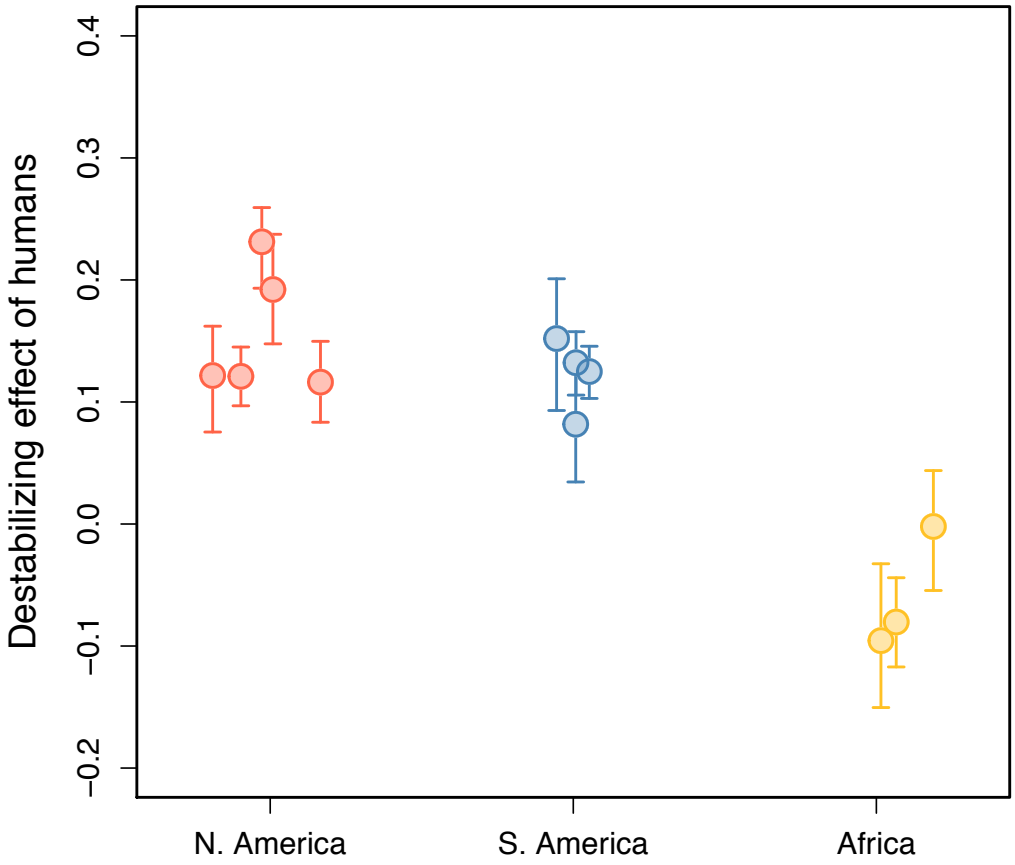

Figure S6 The impact of human arrival when considering extinct species in African large-mammal assemblages. Each point represents the destabilizing effect of humans in a given site. Assemblages from different continents are grouped by the position in the x-axis and colours, as coded in the map. Error bars depict the 95% confidence interval. Values close to zero mean the destabilizing effect of humans would not be greater than the expected effect of an additional small-sized predator.

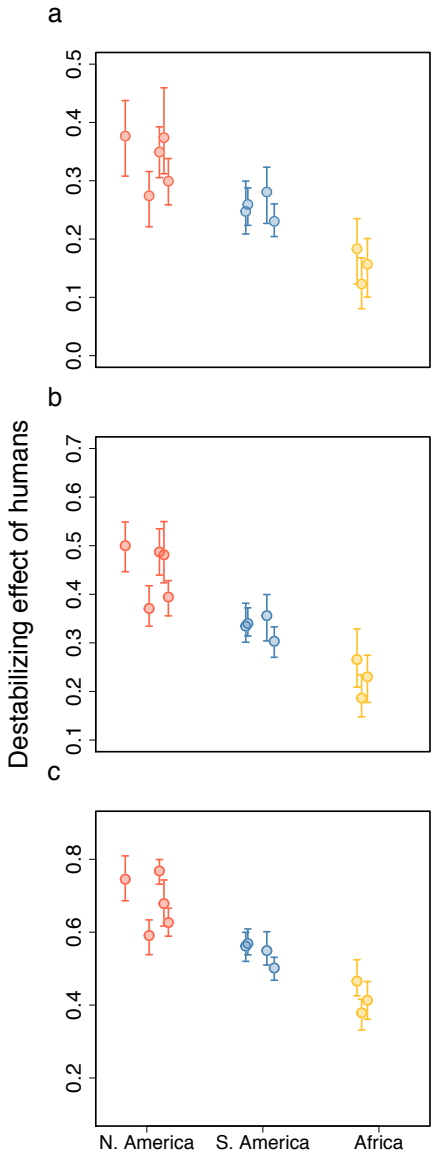

Figure S7 The impact of human arrival when considering humans directly impacted the populations of other predators. Each point represents the destabilizing effect of humans in a given site. The mean strength of interactions between humans and other predators was (a) half, (b) equal, (c) or twice as large as the mean impact of predators on herbivores. Assemblages from different continents are grouped by the position in the x-axis and colours. Error bars depict the 95% confidence interval. Values close to zero mean the destabilizing effect of humans would not be greater than the expected effect of an additional small-sized predator.

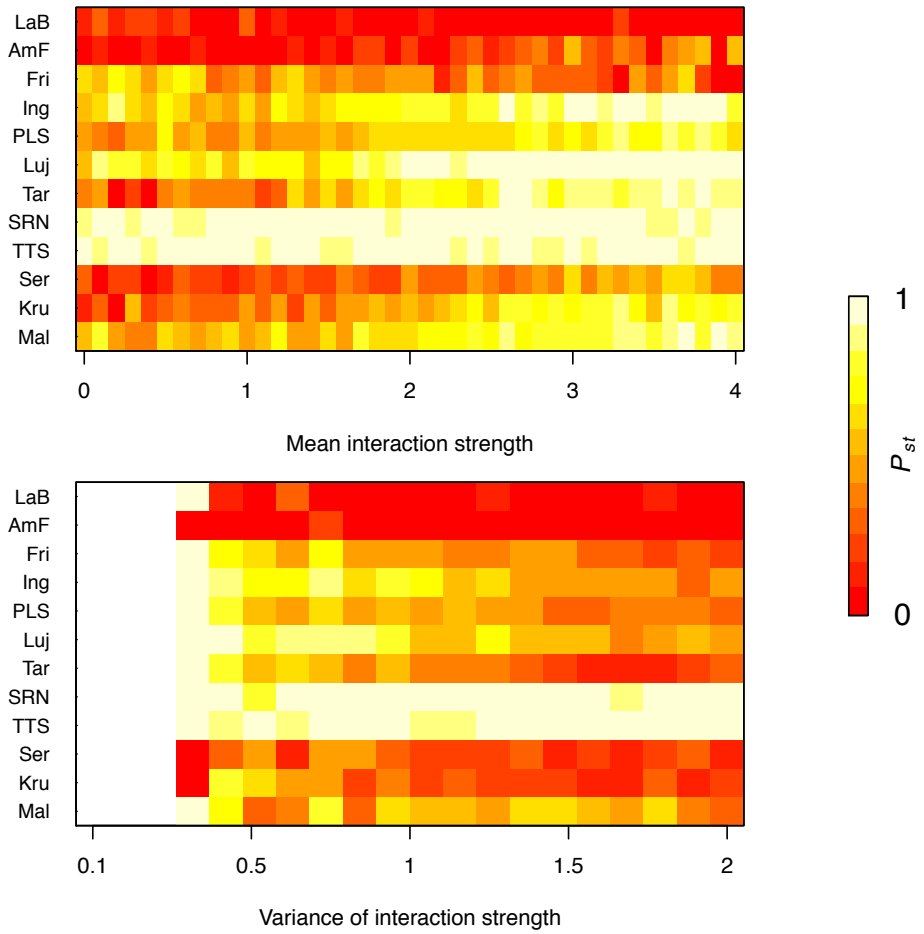

Figure S8 Sensitivity of P_{st} to changes in the mean and variance of interaction strength. Each element of the grid shows the relative P_{st} (normalized taking into account the maximum and minimum values for each μ or σ value) of each analysed large-mammal assemblage.

Supplementary Tables

Table S1 Information on the Pleistocene and modern sites used. N_{pred} and N_{prey} are the richness of predator and prey species in each assemblage.

Site	Location	N_{pred}	N_{prey}	Time range
N. America (Pleistocene)				
La Brea Tar Pits (Pit 91) [38]	California, USA	8	12	0.1-0.01 Ma
American Falls area [39, 40]	Idaho, USA	7	15	0.1-0.01 Ma
Friesenhahn Cave [41, 42]	Texas, USA	6	9	0.02-0.01 Ma
Ingleside [43]	Texas, USA	5	17	0.01-0.01 Ma
Page-Ladson Site (Aucilla River) [44]	Florida, USA	5	15	0.01-0.01 Ma
S. America (Pleistocene)				
Luján – Guerrero Member [45, 46]	Buenos Aires, Argentina	5	23	0.8-0.01 Ma
Tarija Basin [47, 48]	Tarija, Bolivia	6	23	0.04-0.02 Ma
São Raimundo Nonato [49]	Piauí, Brazil	3	13	0.1-0.01 Ma
Talara Tar Seeps [50]	Talara Region, Peru	3	9	0.1-0.01 Ma
Africa (modern)				
Serengeti National Park [51]	N Tanzania	5	16	Modern
Kruger National Park [29]	NE South Africa	5	22	Modern
Mala Mala Reserve [52]	NE South Africa	4	18	Modern

Table S2 Nestedness (*NODF*) and modularity (*M*) of large-mammal assemblages. *N** and *M** are the relative nestedness and modularity obtained according to eq. 5.

Site	*NODF*	*M*	*N**	*M**
N. America (Pleistocene)				
La Brea Tar Pits (Pit 91)	79.82±4.09	0.13±0.03	0.31±0.14	0.02 ± 0.21
American Falls area	75.48±4.87	0.13±0.03	0.33±0.10	-0.08 ± 0.21
Friesenhahn Cave	78.62±6.20	0.16±0.03	0.36±0.13	-0.15 ± 0.19
Ingleside	80.53±6.62	0.14±0.03	0.30±0.10	-0.12 ± 0.20
Page-Ladson Site (Aucilla River)	72.15±5.47	0.15±0.03	0.27±0.07	-0.08 ± 0.21
S. America (Pleistocene)				
Luján – Guerrero Member	73.34±3.65	0.17±0.04	0.37±0.13	-0.08 ± 0.21
Tarija Basin	61.92±8.99	0.11±0.04	0.44±0.9	-0.13 ± 0.19
São Raimundo Nonato	53.33±10.83	0.09±0.04	0.012±0.13	-0.01 ± 0.39
Talara Tar Seeps	77.30±4.92	0.17±0.04	0.08±0.15	-0.02 ± 0.48
Africa (modern)				
Serengeti National Park	73.84	0.10	0.15	-0.12
Kruger National Park	61.99	0.07	0.01	-0.21
Mala Mala Reserve	74.07	0.16	0.27	-0.01

Table S3 Probability of stability (P_{st}) for community matrices representing each site. Columns represent different methods of assigning interaction strengths. Confidence intervals within parentheses.

	P_{st}		
	Random	Asymmetric	Body mass
N. America (Pleistocene)			
La Brea Tar Pits	0.23 (0.21-0.25)	0.68 (0.65-0.71)	0.53 (0.50-0.56)
American Falls area	0.21 (0.18-0.24)	0.64 (0.61-0.67)	0.48 (0.45-0.51)
Friesenhan Cave	0.45 (0.43-0.48)	0.83 (0.81-0.85)	0.73 (0.70-0.73
Ingleside	0.51 (0.47-0.54)	0.85 (0.83-0.87)	0.69 (0.66-0.68)
Page-Ladson Site	0.42 (0.50-0.45)	0.80 (0.78-0.83)	0.65 (0.62-0.67)
S. America (Pleistocene)			
Luján – Guerrero Member	0.55 (0.52-0.58)	0.88 (0.86-0.90)	0.60 (0.58-0.61)
Tarija Basin	0.35 (0.32-0.38)	0.78 (0.75-0.80)	0.48 (0.45-0.51)
São Raimundo Nonato	0.75 (0.72-0.78)	0.93 (0.92-0.95)	0.89 (0.87-0.91)
Talara Tar Seeps	0.78 (0.73-0.80)	0.95 (0.93-0.96)	0.90 (0.89-0.91)
Africa (modern)			
Serengeti National Park	0.28 (0.25-0.31)	0.68 (0.65-0.71)	0.50 (0.48-0.52)
Kruger National Park	0.30 (0.27-0.33)	0.72 (0.69-0.74)	0.50 (0.47-0.53)
Mala Mala Reserve	0.45 (0.42-0.48)	0.79 (0.77-0.82)	0.66 (0.63-0.69)

Table S4 Average time to return to equilibrium (τ) for community matrices representing each site. Columns represent different methods of assigning interaction strengths. Confidence intervals within parentheses.

	τ		
	Random	Asymmetric	Body mass
N. America (Pleistocene)			
La Brea Tar Pits	5.12 (4.69-5.64)	3.36 (3.21-3.53)	3.58 (3.38-3.78)
American Falls area	5.39 (5.00-5.86)	3.27 (3.08-3.46)	3.51 (3.31-3.71)
Friesenhan Cave	3.69 (3.49-3.90)	2.41 (2.31-2.50)	2.56 (2.45-2.67)
Ingleside	4.29 (4.05-4.57)	1.91 (1.84-1.98)	2.12 (2.03-2.21)
Page-Ladson Site	4.28 (4.02-4.57)	2.14 (2.07-2.22)	2.30 (2.19-2.41)
S. America (Pleistocene)			
Luján – Guerrero Member	4.95 (4.68-5.25)	1.77 (1.71-1.82)	2.41 (2.28-2.54)
Tarija Basin	6.19 (5.71-6.76)	2.31 (2.20-2.41)	2.95 (2.78-3.12)
São Raimundo Nonato	3.24 (3.12-3.37)	1.26 (1.23-1.29)	1.23 (1.20-1.26)
Talara Tar Seeps	2.63 (2.54-2.73)	1.30 (1.27-1.33)	1.32 (1.28-1.36)
Africa (modern)			
Serengeti National Park	4.75 (4.42-5.14)	2.47 (2.34-2.60)	2.64 (2.47-2.81)
Kruger National Park	5.46 (5.10-5.88)	2.28 (2.18-2.38)	2.64 (2.50-2.78)
Mala Mala Reserve	4.49 (4.21-4.81)	1.80 (1.73-1.87)	1.82 (1.75-1.89)

Table S5 Results of regression models for P_{st}. Each column represents a different method of assigning interaction strengths in the community matrix. The last column shows the results while assuming Lotka-Volterra model with self-limitation of prey where only feasible equilibrium points were considered. Rows show the F-statistic, the determination coefficient (R^2), and estimates for each model parameter (K_{pred} and K_{prey} are the richness of predator and prey species; m_{pred} and m_{prey} are the average body mass of predators and prey species; N* and M* are the average relative nestedness and modularity). * $p < 0.05$; ** $p < 0.001$; *** $p < 0.001$.

	Random	Asymmetric	Body mass	LV
F	55.36***	33.94***	41.16***	39.8***
R^2	0.90	0.85	0.91	0.87
K_{pred}	-116.14***	-64.13***	-77.46***	-130.50***
K_{prey}	_	_	-14.96***	15.23**
m_{pred}	_	_	_	_
m_{prey}	321.26***	202.74**	173.081**	_
N*	_	_	_	_
M*	_	_	_	_

Table S6 Results of regression models for τ. Each column represents a different method of assigning interaction effects in the community matrix. The last column shows the results while assuming Lotka-Volterra model with self-limitation of prey where only feasible equilibrium points were considered. Rows show the F-statistic, the determination coefficient (R^2), and estimates for each model parameter (K_{pred} and K_{prey} are the richness of predator and prey species; m_{pred} and m_{prey} are the average body mass of predators and prey species; N* and M* are the average relative nestedness and modularity). * $p < 0.05$; ** $p < 0.001$; *** $p < 0.001$.

	Random	Asymmetric	Body mass	LV
F	68.85***	63.69***	130.00***	29.83***
R^2	0.92	0.91	0.92	0.84
K_{pred}	0.42***	0.10***	0.48***	135.48***
K_{prey}	0.14***	_	_	-23.00***
m_{pred}	_	_	_	_
m_{prey}	_	-0.16**	_	_
N*	_	_	_	_
M*	_	_	_	_

Table S7 Pleistocene large mammals (and estimated body mass) in East and Southern Africa. Data from refs. [37, 53].

	Body mass (kg)
Eastern Africa	
Syncerus antiquus	1000
Damaliscus hypsodon	150
Southern Africa	
Equus capensis	400
Syncerus antiquus	1000
Megalotragus priscus	350
Antidorcas australis	40
Antidorcas bondi	34

Table S8 Comparison of P_{st} estimates derived using two different methods. P_{st} and averaged P_{st} over 100 potential matrices built from the same underlying predator-prey network ($\overline{P}_{st}$). Interaction strength assignment as a function of body mass.

	P_{st}	$\overline{P}_{st}$
N. America (Pleistocene)		
La Brea Tar Pits	0.53 (0.50-0.56)	0.52
American Falls area	0.48 (0.45-0.51)	0.47
Friesenhan Cave	0.73 (0.70-0.73	0.72
Ingleside	0.69 (0.66-0.68)	0.67
Page-Ladson Site	0.65 (0.62-0.67)	0.67
S. America (Pleistocene)		
Luján – Guerrero Member	0.60 (0.58-0.61)	0.59
Tarija Basin	0.48 (0.45-0.51)	0.51
São Raimundo Nonato	0.89 (0.87-0.91)	0.88
Talara Tar Seeps	0.90 (0.89-0.91)	0.91
Africa (modern)		
Serengeti National Park	0.50 (0.48-0.52)	0.53
Kruger National Park	0.50 (0.47-0.53)	0.49
Mala Mala Reserve	0.66 (0.63-0.69)	0.66

Supplementary References

1. Marean CW, Ehrhardt CL. 1995 Paleoanthropological and paleoecological implications of the taphonomy of a sabertooth's den. *J. Hum. Evol.* **29**, 515-547.
2. Van Valkenburgh B. 2006 Evolution of feeding morphologies in the Carnivora. *Integr. Comp. Biol.* **46**, 147-163.

3. Koch PL, Hoppe KA, Webb SD. 1998 The isotopic ecology of late Pleistocene mammals in North America - Part 1. Florida. *Chem. Geol.* **152**, 119-138.
4. Yeakel J, Guimarães PR, Bocherens H, Koch PL. 2013 The impact of climate change on the structure of Pleistocene food webs across the mammoth steppe. *Proc. R. Soc. B* **280**, 20130239.
5. Coltrain JB, Harris JM, Cerling TE, Ehleringer JR, Dearing MD, Ward J, Allen J. 2004 Rancho La Brea stable isotope biogeochemistry and its implications for the palaeoecology of late Pleistocene, coastal southern California. *Palaeogeogr. Palaeoclimatol. Palaeoecol.* **205**, 199-219.
6. Fox-Dobbs K, Bump JK, Peterson RO, Fox DL, Koch PL. 2007 Carnivore-specific stable isotope variations and variation in foraging ecology of modern and ancient wolf populations: case studies from Isle Royale, Minnesota, and La Brea. *Can. J. Zool.* **85**, 458-471.
7. Fariña RA, Vizcaíno SF, De Iuliis G, Tambusso S. 2013 *Megafauna: giant beasts of Pleistocene South America (Life of the Past)*. Bloomington, Indiana University Press.
8. Prevosti FJ, Martin FM. 2013 Paleoecology of the mammalian predator guild of Southern Patagonia during the latest Pleistocene: Ecomorphology, stable isotopes, and taphonomy. *Quatern. Int.* **305**, 74-84.
9. Prevosti FJ, Palmqvist P. 2001 Análisis ecomorfológico del cánido hipercarnívoro *Theriodictis platensis* Mercerat (Mammalia, Carnivora), basado en un nuevo ejemplar del Pleistoceno de Argentina. *Ameghiniana* **38**, 375-384.
10. Prevosti FJ, Vizcaíno SF. 2006 Paleoecology of the large carnivore guild from the late Pleistocene of Argentina. *Acta Palaeontol. Pol.* **51**, 407-422.

11. Anderson CR, Lindzey FG. 2003 Estimating cougar predation rates from GPS location clusters. *J. Wildlife Manage.* **67**, 307-316.

12. Bartnick TD, Van Deelen TR, Quigley HB, Craighead D. 2012 Variation in cougar (*Puma concolor*) predation habits during wolf (*Canis lupus*) recovery in the southern Greater Yellowstone Ecosystem. *Can. J. Zool.* **91**, 82-93.

13. Foster RJ, Harmsen BJ, Valdes B, Pomilla C, Doncaster CP. 2009 Food habits of sympatric jaguars and pumas across a gradient of human disturbance. *J. Zool.* **280**, 309-318.

14. Crawshaw PG, Quigley HB. 2002 Jaguar and puma feeding habits in the Pantanal, Brazil, with implications for their management and conservation. In *El jaguar en el nuevo milenio* (eds. Medellin RA, Equihua C, Chetkiewicz C), pp. 223-235. New York, Wildlife Conservation Society.

15. Van Valkenburgh B, Hertel F. 1993 Tough times at La Brea: Tooth breakage in large carnivores of the Late Pleistocene. *Science* **261**, 456-460.

16. Fox-Dobbs K, Leonard JA, Koch PL. 2008 Pleistocene megafauna from eastern Beringia: Paleoecological and paleoenvironmental interpretations of stable carbon and nitrogen isotope and radiocarbon records. *Palaeogeogr. Palaeoclimatol. Palaeoecol.* **261**, 30-46.

17. Williams RJ, Anandanadesan A, Purves D. 2010 The probabilistic niche model reveals the niche structure and role of body size in a complex food web. *PLoS One* **5**, e12092.

18. Pires MM, Guimarães PR. 2013 Interaction intimacy organizes networks of antagonistic interactions in different ways. *J. Royal Soc. Interface* **10**, 20120649.

19. Allesina S, Tang S. 2012 Stability criteria for complex ecosystems. *Nature* **483**, 205-208.

20. Wootton JT, Emmerson M. 2005 Measurement of interaction strength in nature. *Annu. Rev. Ecol. Evol. Syst.* **36**, 419-444.

21. Pimm SL, Lawton JH. 1978 On feeding on more than one trophic level. *Nature* **275**, 542-544.

22. Emmerson M, Yearsley JM. 2004 Weak interactions, omnivory and emergent food-web properties. *Proc. R. Soc. B* **271**, 397-405.

23. Woodward G, Ebenman B, Emmerson M, Montoya JM, Olesen JM, Valido A, Warren PH. 2005 Body size in ecological networks. *Trends Ecol. Evol.* **20**, 402-409.

24. Brose U, Ehnes RB, Rall BC, Vucic-Pestic O, Berlow EL, Scheu S. 2008 Foraging theory predicts predator-prey energy fluxes. *J. Anim. Ecol.* **77**, 1072-1078.

25. Yoder JB, Nuismer SL 2010 When does coevolution promote diversification? *Am. Nat.* **176**, 802-817.

26. Nuismer SL, Gomulkiewicz R, Ridenhour BJ. 2010 When is correlation coevolution? *Am. Nat.* **175**, 525-537.

27. Houston DC. 1979 The adaptations of scavengers. In *Serengeti, dynamics of an ecosystem* (eds. Sinclair ARE, Griffiths MN), pp. 263-286. Chicago, Univ. of Chicago Press.

28. Macdonald DW. 1983 The ecology of carnivore social-behavior. *Nature* **301**, 379-384.

29. Owen-Smith N, Mills MGL. 2008 Predator-prey size relationships in an African large-mammal food web. *J. Anim. Ecol.* **77**, 173-183.

30. Yeakel JD, Guimarães PR, Novak M, Fox-Dobbs K, Koch PL. 2012 Probabilistic patterns of interaction: the effects of link-strength variability on food web structure. *J. R. Soc. Interface* **9**, 3219-3228.

31. Treves A, Naughton-Treves L. 1999 Risk and opportunity for humans coexisting with large carnivores. *J. Hum. Evol.* **36**, 275-282.

32. Rohr RP, Saavedra S, Bascompte J. 2014 On the structural stability of mutualistic systems. *Science* **345**, 1-9.

33. McCann KS. 2011 *Food Webs*. Princeton, Princeton University Press.

34. Weitz JS, Levin SA. 2006 Size and scaling of predator-prey dynamics. *Ecol. Lett.* **9**, 548-557.

35. R Core Team. 2014 A language and environment for statistical computing. R Foundation for Statistical Computing, Vienna, Austria. *URL: http://www.R-project.org/.*

36. Klein RG. 1984 Mammalian extinctions and stone age people in Africa. In *Quaternary extinctions: a prehistoric revolution* (eds. Martin PS, Klein RG), pp. 553-573, Tucson, The University of Arizona Press.

37. Faith JT, Tryon CA, Peppe DJ, Fox DL. 2013 The fossil history of Grévy's zebra (*Equus grevyi*) in equatorial East Africa. *J. Biogeogr.* **40**, 359-369.

38. Friscia AR, Van Valkenburgh B, Spencer L, Harris J. 2008 Chronology and spatial distribution of large mammal bones in PIT 91, Rancho La Brea. *Palaios* **23**, 35-42.

39. Pinsof JD. 1998 The American Falls local fauna: Late Pleistocene (Sangamonian) vertebrates from southeastern Idaho. *Idaho Museum of Natural History Occasional Paper* **36**, 121-145.

40. Hopkins ML, Bonnichsen R, Fortsch D. 1969 The stratigraphic position and faunal associates of *Bison* (*Gigantobison*) *latifrons* in southeastern Idaho. *Tebiwa* **12**, 1-8.

41. Toomey RS. 1994 Vertebrate paleontology of Texas caves In *The caves and karst of Texas* (eds. Elliot WR, Veni G), pp. 69-83. Huntsville, National Speleological Society.

42. Graham RW. 1976 Pleistocene and holocene mammals, taphonomy, and paleoecology of the Friesenhahn Cave local fauna, Bexar County, Texas. Austin, University of Texas.

43. Lundelius Jr. EL. 1972 *Fossil vertebrates from the late Pleistocene Ingleside fauna, San Patricio County, Texas*. Austin, Bureau of Economic Geology, University of Texas at Austin

44. Webb SD. 2006 *First floridians and last mastodons: The Page-Ladson Site in the Aucilla River*. Dordrecht, Springer.

45. Tonni EP, Prado JL, Menegaz AN, Salemme MC. 1985 La Unidad Mamífero (Fauna) Lujanense. Proyección de la estratigrafía mamaliana al Cuaternario de la Región Pampeana. *Ameghiniana* **22**, 255-261.

46. Tonni EP, Huarte RA, Carbonari JE, Figini AJ. 2003 New radiocarbon chronology for the Guerrero Member of the Luján Formation (Buenos Aires, Argentina): palaeoclimatic significance. *Quatern. Int.* **109**, 45-48.

47. Marshall LG, Sempere T. 1991 Fosiles y facies de Bolivia: 1. Vertebrados. *Revista Tecnica de Yacimientos Petroliferos Fiscales Bolivianos* **12**, 631-652.

48. Coltorti M, Abbazzi L, Ferretti MP, Iacumin P, Rios FP, Pellegrini M, Pieruccini P, Rustioni M, Tito G, Rook L. 2007 Last Glacial mammals in South America: a new scenario from the Tarija Basin (Bolivia). *Naturwissenschaften* **94**, 288-299.

49. Guêrin C. 1991 The upper Pleistocene vertebrate fauna from the archaeological area of São-Raimundo Nonato (Piauí, Brazil). *CR Acad. Sc. Paris* **312**, 567-572.

50. Lemon RRH, Churcher CS. 1961 Pleistocene geology and paleontology of the Talara Region, Northwest Peru. *Am. J. Sci.* **259**, 410-429.

51. Baskerville EB, Dobson AP, Bedford T, Allesina S, Anderson TM, Pascual M. 2011 Spatial guilds in the Serengeti food web revealed by a bayesian group model. *PLoS Comput. Biol.* **7**, 1002321.

52. Radloff FGT, Du Toit JT. 2004 Large predators and their prey in a southern African savanna: a predator's size determines its prey size range. *J. Anim. Ecol.* **73**, 410-423.

53. Faith JT. 2013 Late Pleistocene and Holocene mammal extinctions on continental Africa. *Earth-Sci. Rev.* **128**, 105-121.